Similarity Relations of Process Variables in Resin Flow of RTM Process

Moon-Kwang Um[1], Joon-Hyung Byun[1] and Isaac M. Daniel[2]

[1] Korea Institute of Machinery and Materials, Composite Materials Laboratory, 66 Sangnam-dong, Changwon, 641- 010, South Korea
[2] Robert R. McCormick School of Engineering and Applied Science, Center for Intelligent Processing of Composites, Northwestern University, Evanston, IL 60208, USA

ABSTRACT

Liquid molding processes, such as resin transfer molding, involve resin flow through a porous medium inside a mold cavity. Numerical analysis of resin flow and mold filling is a very useful means for optimization of the manufacturing process. However, numerical analysis is very time consuming and requires a great deal of effort, since a new numerical calculation is needed for every set of material properties, part size and injection conditions. The effort is appreciably reduced by using similarity solutions instead of repeated numerical calculations. In this study, the similarity relations for pressure, resin velocity and flow front propagation are proposed for predicting results for new cases based on the numerical simulation for one specific case. The model gives a correlation of flow induced variables between two different cases. The model was verified by comparing results obtained by the similarity relations and by independent numerical simulation.

1. INTRODUCTION

In the liquid molding process of composites, numerical analysis of mold filling is a useful and necessary means of process optimization, such as determination of gate/vent locations and their opening-closing sequence, injection pressure and flow rate. The analysis also helps in the selection of a suitable material system. For simple geometries, analytic solutions can be used to estimate the mold filling pattern [1,2]. However, in many cases of realistic and complex geometries numerical methods have been employed to obtain accurate solutions. Various numerical schemes, such as the finite difference method [3,4], the boundary element method [5,6] and the finite element method [7-17] have been adopted and tested. At the present, a control volume based finite element method (CVFEM) is a widely accepted method due to its relative ease of implementation and effectiveness in treating the moving flow front without mesh regeneration.

In general, a great deal of effort is necessary to perform a numerical analysis as it requires mesh generation, input data preparation, post processing of the result, etc. However, the effort is appreciably reduced by using similarity solutions which obviate the need for repeated simulations. In this paper, similarity relations of variables induced in resin flow are proposed to obtain multiple results for many cases based on data from only one numerical analysis.

2. SIMILARITY RELATIONS

The conservation of momentum for resin flow through a fiber preform is described by the well-known Darcy's law [18]. Darcy's law is a kind of simplified form of the Navier-Stokes equation for resin flow through porous media. The flow through porous media is assumed to be a low Reynolds number flow where the inertia force is negligible and the pressure force balances the viscous force.

$$\bar{u}_D = -\frac{[K]}{\mu}\nabla P \tag{1}$$

where $\bar{u}_D$ is a Darcian velocity, [K] the permeability matrix of the reinforcement, P pressure, ∇P its gradient, and μ the resin viscosity. Here, the resin is assumed to be an incompressible Newtonian liquid. Actually, the Darcian velocity is an imaginary velocity and the real velocity that we observe in mold filling is an apparent or pore velocity ($\bar{u}_P$) defined as

$$\bar{u}_P = \frac{\bar{u}_D}{\varepsilon} = -\frac{[K]}{\varepsilon\mu}\nabla P \tag{2}$$

where $\varepsilon = 1 - \mathrm{V_f}$ (porosity), $\mathrm{V_f}$ = fiber volume ratio

The governing equation of resin flow is obtained by substituting the apparent velocity into the mass conservation equation

$$\nabla \cdot \bar{u}_P = \nabla \cdot \left(-\frac{[K]}{\varepsilon\mu}\nabla P \right) = 0 \tag{3}$$

If the partial differential equation is linear and homogeneous, the solution obtained for the given material properties, the part geometry and the boundary conditions, is also a solution for the case where all these parameters are changed. The existence of a similarity solution is deduced from the fact that the governing equation (Eq.3) is linear and homogeneous. Also, the analogy of flow front shapes shown in the cases where the properties and the conditions are different guarantees the existence of similarity solutions. The boundary conditions for solving the pressure field are summarized as follows

$$\text{Injection Gate}: P = P_i(t) \tag{4}$$

$$\text{Mold Wall}: \frac{\partial P}{\partial n} = 0 \tag{5}$$

$$\text{Flow Front}: \mathrm{P} = 0 \tag{6}$$

where $P_i(t)$ is the pressure at the gate and n denotes the direction normal to the mold wall.

When the flow is assumed to be quasi-steady, the pressure field is obtained by solving the governing differential equation (Eq.3) with the given boundary conditions (Eqs. 4-6). The solution technique can be either analytical or numerical. For example, the solution of the pressure field can be determined through the variational or weak formulation of Eq.3 and application of the boundary conditions,

$$\iiint_R w\nabla \cdot \bar{u}_P dV = \iiint_R w\nabla \cdot \left(\frac{[K]}{\varepsilon\mu}\nabla P \right) dV = 0 \tag{7}$$

where w is a weight function, R the region filled with resin and V the volume. With the aid of the pressure field obtained by Eq. 7, the velocity field at that instant is calculated from Eq. 2. Then, the flow front is advanced with the resin velocity and the same procedure is repeated for the newly filled region. To derive similarity relations, additional assumptions are made as follows:

- In general, the viscosity changes as chemical reaction progresses. The resin is premixed and then injected into the mold. The mixed resin experiences the same temperature history throughout the process. Therefore, the viscosity at the specific instant of mold fill is uniform throughout the impregnated region.
- The drag force induced by the flow does not cause distortion of the perform, thus, the permeability does not change during the flow.

2.1 Pressure and its Gradient

As a first step in mold filling analysis the pressure field must be determined in the impregnated region. The material properties, part geometry and injection pressure for driving the model are defined in Table 1 and Fig. 1. When the resin is injected through multiple gates, the ratios of injection pressures at the gates in the original problem should be equal to those in the sample problem to maintain the analogy of flow front shape between the two cases. This is an important requirement for the existence of a similarity solution for multiple-gate injection.

$$\frac{P_{o,k}(t)}{P_{o,1}(t)} = \frac{P_{s,k}(t)}{P_{s,1}(t)} \qquad (2 \le k \le l) \tag{8}$$

where, $P_{o,1}(t)$ and $P_{s,1}(t)$ are the first gates in the original and sample cases where the resin is injected into the mold. In the case of sequentially opened multiple gates, the open time at each gate should also be adjusted in the sample problem and it will be described in detail in the "time scale transformation" section below. In the case of a single gate, the gate open time and the ratio of pressures are not required for development of the model.

Applying Eq.7 to *m* components of reinforcement filled with resin at a specific instant in the original problem (Fig. 1), we obtain

$$\iiint_{R_1} w\nabla\cdot(\frac{[K]_{o,1}}{\varepsilon_{o,1}\mu_o(t)}\nabla P)dV + \ldots + \iiint_{R_m} w\nabla\cdot(\frac{[K]_{o,m}}{\varepsilon_{o,m}\mu_o(t)}\nabla P)dV$$

$$= \frac{1}{\mu_o(t)}\sum_{j=1}^{m}\left\{\iiint_{R_j} w\nabla\cdot(\frac{[K]_{o,j}}{\varepsilon_{o,j}}\nabla P)dV\right\} = 0 \qquad (1 \le m \le n) \tag{9}$$

where R_j is the *j*-th component of reinforcement in the impregnated region. Here, we assume the solution of the pressure field at the *j*-th reinforcement component as

$$\text{Solution of pressure field} = [P(\mathbf{X}_{o,j}, t_o)]_{sol} \qquad 1 \le j \le m \tag{10}$$

where $\mathbf{X}_{o,j}$ is the position vector defining the *j*-th reinforcement and t_o the time scale in the original problem.

Applying Eq. 7 to the filled region in the sample case by analogy with the original, we obtain

$$\frac{1}{\mu_s(t)}\sum_{j=1}^{m}\left\{\iiint_{R_j^*} w\nabla\cdot(\frac{[K]_{s,j}}{\varepsilon_{s,j}}\nabla P)dV^*\right\} = 0 \qquad (1 \le m \le n) \tag{11}$$

where R_j^* is the *j*-th reinforcement component of the sample case and Eq. 11 is a volume integral in the sample. The above integral can be transformed into that of the original case by introducing the Jacobian cubic (a_L^3) and the scale factors a_K and a_ε accounting for the permeability and porosity effects on the transformation.

$$\frac{a_K a_L^3}{a_\varepsilon}\frac{1}{\mu_s(t)}\sum_{j=1}^{m}\left\{\iiint_{R_j} w\nabla\cdot(\frac{[K]_{o,j}}{\varepsilon_{o,j}}\nabla P)dV\right\}=0 \qquad (1\le m\le n) \qquad (12)$$

The integral part of Eq. 12 is the same as that of Eq. 9. Therefore, based on the linearity and homogeneity of the governing equation, the solution of Eq. 12 is determined by the ratio of injection boundary conditions between the two cases. This ratio can be described by the pressure at the first gates, $P_{o,1}(t_o)$ and $P_{s,1}(t_s)$, which are representative of the two cases (Eq. 8). The relation between t_o and t_s is explained below in the "time scale transformation" section. The solution of Eq. 12, the pressure field, and its gradient are described as follows by considering Eq. 10 and Table 1.

$$[P(\mathbf{X}_{s,j},t_s)]_{sol}=\frac{P_{s,1}(t_s)}{P_{o,1}(t_o)}[P(\mathbf{X}_{o,j},t_o)]_{sol} \qquad 1\le j\le m \qquad (13)$$

$$[\nabla P(\mathbf{X}_{s,j},t_s)]_{sol}=\frac{1}{a_L}\frac{P_{s,1}(t_s)}{P_{o,1}(t_o)}[\nabla P(\mathbf{X}_{o,j},t_o)]_{sol} \qquad 1\le j\le m \qquad (14)$$

where $\mathbf{X}_{s,j}$ is a position vector of the *j*-th reinforcement component in the sample problem. Finally, Eqs. 13 and 14 represent similarity relations of pressure and its gradient between the original and the sample cases at a specific instant of mold fill. It is known from Eqs. 13 and 14 that the similarities of pressure and its gradient are dependent on the injection pressure ratio and the part size scale factor.

2.2 Resin Velocity

Resin flow is induced by the pressure gradient developed in the flow field and the gradient determines the resin penetrating velocity through the porous medium. Therefore, the obtained pressure gradient is used to determine resin velocity (Eq. 2). The apparent resin velocity in the flow region of the original case can be rewritten as

$$\bar{u}_p(\mathbf{X}_{o,j},t_o)=-\frac{[K]_{o,j}}{\mu_o(t_o)\varepsilon_{o,j}}[\nabla P(\mathbf{X}_{o,j},t_o)]_{sol} \qquad (1\le j\le m) \qquad (15)$$

For the flow front shape of the sample which has an analogy with that of the original, resin velocity is expressed as follows with the aid of the scaling factors of material property, viscosity, injection pressure and velocity of the original problem.

$$\begin{aligned}\bar{u}_p(\mathbf{X}_{s,j},t_s)&=-\frac{[K]_{s,j}}{\mu_s(t_s)\varepsilon_{s,j}}[\nabla P(\mathbf{X}_{s,j},t_s)]_{sol,j}\\&=\frac{a_K}{a_\varepsilon a_L}\frac{\mu_o(t_o)}{\mu_s(t_s)}\frac{P_s(t_s)}{P_o(t_o)}\bar{u}_p(X_{o,j},t_o) \qquad (1\le j\le m)\end{aligned} \qquad (16)$$

Equation 16 is the final form of resin velocity similarity between the original and the sample problems at a specific instant of mold fill. It is shown from Eq. 16 that the similarity of resin velocites depends upon all the material properties, part size and injection boundary conditions.

2.3 Time Scale Transformation

It is deduced from the similarity of flow front shapes that there is only a change of time scale between corresponding points on the flow fronts. The time transformation is formulated as follows. As a starting point, the similarity of resin velocity, Eq. 16, is resolved into displacement (*S*) and time expressed as

$$\frac{\mu_o(t_o)}{\mu_s(t_s)}\frac{P_{s,1}(t_s)}{P_{o,1}(t_o)}\frac{dt_s}{dt_o}=\frac{a_\varepsilon a_L}{a_K}\frac{dS_{s,j}}{dS_{o,j}} \qquad (1\le j\le m) \tag{17}$$

The flow fronts for the two cases at a specific time match exactly by applying the part geometrical scale factor (a_L) to the displacement because the flow front is a time integral of the displacement.

$$S_{s,j}=a_L S_{o,j} \qquad (1\le j\le m) \tag{18}$$

By replacing Eq. 17 with Eq. 18 and integrating it with respect to time, the transformation rule gives

$$\int_0^{t_s}\frac{P_s(t)}{\mu_s(t)}dt=\frac{a_\varepsilon a_L^2}{a_K}\cdot\int_0^{t_o}\frac{P_o(t)}{\mu_o(t)}dt \tag{19}$$

The relation between time scales t_o and t_s in Eqs.13-15 is determined by Eq. 19. This equation is the time scale transformation for flow fronts between the original and the sample case. It is known from Eq. 19 that the similarity in time scales is also dependent on all the material properties, part size and injection boundary conditions.

3. NUMERICAL SCHEME

Resin flow can be predicted by means of experimental, analytical or numerical methods. The most powerful method for solving a real problem is numerical analysis. Therefore, a numerical scheme was applied to verify the suggested similarity relations. A numerical formulation was performed for a three-dimensional shell structure, which is locally a two-dimensional case. Of course, the similarity model is valid for mold filling of fully three-dimensional structures.

The region filled with resin or the calculation domain changes as the flow front proceeds. The proper description of the domain filled with resin is very important because it plays a crucial role in the accurate prediction of the flow front and the related physical parameters. In general, there can be two choices for a grid system, a moving grid or a fixed grid. In this work, the fixed grid system the grids generated at the beginning are used throughout the calculation. It greatly relieves the burden of node regeneration.

The numerical scheme was verified by comparing the calculated and predicted complete fill times for the injection condition of constant flow rate in the original problem. Resin was injected through Gate 1 (Fig. 2). The calculated fill time for the part volume of $2.064\text{x}10^{-4}$ m^3, preform porosity of 0.5 and flow rate of $1.0 \text{ x } 10^{-5}$ m^3/s is 10.32 sec, whereas that determined by numerical simulation is 10.30 sec for an error of approximately 0.20%.

4. VERIFICATION AND DISCUSSION

As already mentioned, the suggested similarity model can predict mold filling of fully three-dimensional geometries. Numerical simulations for locally 2-dimensional shell structures, however, were performed to simplify the verification. The part shape, the generated mesh and the elements are shown in Fig. 2. The node and element numbers in the original case are 513 and 936, respectively. The same node and element numbers are used in the sample case. The dimensions of the original shell structure are 0.3 x 0.2 x 0.08 m and the thickness of the part is 0.003 m. The sample part is magnified by a scale factor $a_L = 2$ with respect to the original. Three different preforms were used and the resin was sequentially injected through two gates. Material properties used in the original case are given in Table 2

and the injection pressure in the original is defined as

$$P_o(t) = \begin{cases} P_{o,1}(t) = 1\times10^5 \ \text{Pa} & \\ P_{o,2}(t) = \begin{cases} 0 & 0 \le t < 30 \\ 1.5\times10^5 \ \text{Pa} & t \ge 30 \end{cases} & \end{cases} \tag{20}$$

The scale factors applied in the transformation from the original to the sample case are

$$a_\varepsilon = 0.25,\ a_K = 0.5,\ a_L = 2 \tag{21}$$

The viscosity in the sample case is

$$\mu_s(t) = 0.7\exp\left[\frac{40}{T_s(t)+273.15} + 0.01t\right] \qquad \text{Pa}\cdot\text{sec} \tag{22}$$

$$\text{where, } T_s(t) = \begin{cases} 20+0.5t & {}^{o}\text{C} \quad 0 \le t \le 100 \\ 70 & {}^{o}\text{C} \quad t \ge 100 \end{cases} \tag{23}$$

The entire quantity of resin has to be premixed before injection and both the resin in the reservoir and that in the mold experience the same temperature history. In general, the viscosity change due to chemical reaction is expressed as a function of temperature and degree of cure [19-20]. For the given cure cycle, however, the viscosity model with temperature and time as variables can be simplified when complete mold filling occurs at an early stage of reaction and the progression of chemical reaction is quite low (Eq. 22). If the temperature history of the injected resin changes, the coefficients of Eq. 22 change. A graphical description of viscosity variation in the original and sample cases is given in Fig. 3. As the verification is performed for multiple gates, Eq. 8 should be satisfied for the existence of similarity and the ratio of first gate pressures at a specific instant is defined as

$$\frac{P_{s,1}(t)}{P_{o,1}(t)} = 3\sqrt{0.02t+0.1} \tag{24}$$

To determine the injection time of the second gate, the time scale transformation is necessary (Eq. 19) and the result is given in Fig. 4. The injection time, 56 sec. in Eq. 25 was determined from Fig. 4. The gate pressures for the sample case are

$$P_s(t) = \begin{cases} P_{s,1}(t) = P_{o,1}(t)\times3\sqrt{0.02t+0.1} \ \text{Pa} & \\ P_{s,2}(t) = \begin{cases} 0 & 0 \le t < 56 \\ P_{o,2}(t)\times3\sqrt{0.02t+0.1} \ \text{Pa} & t \ge 56 \end{cases} & \end{cases} \tag{25}$$

The injection pressures at the two gates of the original and sample cases are shown in Fig. 5.

Using all the properties and conditions defined above, numerical simulations were performed and compared with model predictions. The complete fill times of the original and sample problems were 141.4 sec and 211.9 sec, respectively. The fill time predicted by the model is 211.6 sec and corresponds to an error of about 0.14%. The flow fronts, when matched by the time transformation rule (Fig. 4), are in good agreement as shown in Fig. 6. The pressure fields for the original case at 84.1 sec nearly coincide with those of the sample case at 117.6 sec (Fig. 7, Eq. 26). The velocity fields at 67.9 sec for the original case agree well with those at 99.5 sec for the sample case, although the agreement is not as good as for the flow fronts and pressure fields (Fig. 8, Eq. 27). The slightly increased error does not come from the model, but originates in the numerical scheme used in the study.

$$P_{sol,j}(\mathbf{X}_{s,j},117.6) = 4.6976 \times P_{sol,j}(\mathbf{X}_{o,j},84.1) \qquad 1 \le j \le 3 \qquad (26)$$

$$\overline{u}_p(\mathbf{X}_{s,j},99.5) = 1.8088 \times \overline{u}_p(\mathbf{X}_{o,j},67.9) \qquad 1 \le j \le 3 \qquad (27)$$

The smoothness of the loci lines in Figs. 6-8 can be improved by increasing the number of elements in the simulation. The above results prove the validity of the similarity model.

5. CONCLUSIONS

A new method, the similarity technique, was proposed to predict the resin flow in cases with different material, geometric and process parameters in liquid molding applications based on only one numerical simulation of a reference case. The existence of similarity solutions was deduced from the linearity and homogeneity of the governing partial differential equation. This yields the similarity relations between various cases where the reinforcement properties (permeability and porosity), the resin property (viscosity), the part dimensions and the injection conditions vary. A control volume based finite element method (CVFEM) was incorporated in the calculation of pressure fields, resin velocity and flow front propagation for a given geometry and injection conditions.

The proposed similarity method was verified by matching the numerical results with those predicted by the similarity model. They show good agreement. The result is an appreciable savings in time and effort, by obviating the need for repeated numerical simulations every time the process parameters change. Furthermore, the similarity model is also very useful in optimizing mold filling conditions.

ACKNOWLEDGEMENTS

This research was supported by a grant from the Center for Advanced Materials Processing of the 21st Century Frontier R&D Program and the Advanced Machinery and its Part Development Program funded by the Ministry of Science and Technology, Republic of Korea.

References:

1. Cai, Z., “Simplified mold filling simulation in resin transfer molding”, *J Comp Mater.*, 26(1992), 2606-2630.
2. Boccard A, Lee WI, Springer GS, “Model for determining the vent locations and the fill time of resin transfer molds”, *J Comp Mater.*, 29(1995), 306-333.
3. Coulter, J.P., Smith, B.F., Guceri, S.I., “Experimental and numerical analysis of resin impregnation during the manufacturing of composite materials”, *Proc Amer Soc Comp 2nd Tech Conf*, (1988), 209-217.
4. Trochu, F., Gauvin, R., “Limitations of a boundary fitted finite difference method for the simulation of the resin transfer molding process”, *J Reinf Plast Comp*., 11(1992), 772-786.
5. Um, M.K., Lee, W.I., “A study on the mold filing process in resin transfer molding”, *Polym Eng Sci*, 31(1991), 765-771.
6. Yoo, Y.E., Lee, W.I., “Numerical simulation of the resin transfer mold filling process using the boundary element method”, *Polym Comp*, 17(1996), 368-374.
7. Loos, A.C., MacRae, J.D., “A process simulation model for the manufacture of a blade-stiffened panel by the resin film infusion process”, *Comp Sci Tech*, 56(1996), 273-289.
8. Liu, B., Bickerton, S., Advani, S.G., “Modeling and simulation of resin transfer molding (RTM) - Gate control, venting and dry spot prediction”, *Composites Part A*, 27A(1996), 135-141.
9. Kang, M.K., Lee, W.I., “A flow front refinement technique for the numerical simulation of the resin-transfer molding process”, *Comp Sci Tech*, 59(1999), 1663-1674.
10. Pillai, K.M., Advani, S.G., “Numerical simulation of unsaturated flow in woven fiber preforms during the resin transfer molding process”, *Polym Comp*, 19(1998), 71-80.

11. Bickerton, S., Advani, S.G., "Experimental investigation and flow visualization of the resin transfer mold-filling process in a non-planar geometry", *Comp Sci Tech*, 57(1997), 23-33.
12. Young, W.B., Rupel, K., Han, K., Lee, L.J., Liou, M.J., "Analysis of resin injection molding in molds with preplaced fiber mats. II: Numerical simulation and experiments of mold filling", *Polym Comp*, 12(1991), 30-38.
13. Golestanian, H. and El-Gizawy, A.S., "Physical and numerical modeling of mold filling in resin transfer molding", *Polym Comp*, 19(1998), 395-407.
14. Young, W.B., "Resin flow analysis in the consolidation of multi-directional laminated composites", *Polym Comp*, 16(1995), 250-257.
15. Sun, X., Li, S., Lee, L.J., "Mold filling analysis in vacuum-assisted resin transfer molding. Part I: SCRIMP based on a high-permeable medium", *Polym Comp*, 19(1998), 807-816.
16. Phelan Jr, F.R., Simulation of the injection process in resin transfer molding, *Polym Comp*, 18(1997), 460-476.
17. Gauvin, R. and Trochu, F., "Key issues in numerical simulation for liquid composite molding processes", *Polym Comp*, 19(1998), 233-240.
18. Kaviany, M., *Principles of Heat Transfer in Porous Media*, Springer-Verlag, 1991.
19. Sourour, S. and Kamal, M.R., "Differential scanning calorimetry of epoxy cure: isothermal cure kinetics", *Thermochimica ACTA*, 14(1976), 41-59.
21. Dusi, M.R. and Lee, W.I., Ciriscioli PR, "Springer GS, Cure kinetics and viscosity of Fiberite 976 resin", *J Comp Mater,* 27(1987), 243-261.

Table 1. Material properties, part geometry and injection pressure

		Original	Sample
Reinforcement	Permeability, $[K]$	$[K]_{o,i} \quad (1 \le i \le n)$	$[K]_{s,i} = a_K [K]_{o,i} \quad (1 \le i \le n)$
	Porosity, ε	$\varepsilon_{o,i} \quad (1 \le i \le n)$	$\varepsilon_{s,i} = a_\varepsilon \varepsilon_{o,i} \quad (1 \le i \le n)$
Resin	Viscosity, μ	$\mu_o(t)$	$\mu_s(t)$
Part Shape, $\mathbf{X}$ ($\mathbf{X}$: position vector)		$\mathbf{X}_{o,i} \quad (1 \le i \le n)$ (n : Number of reinforcement)	$\mathbf{X}_s = a_L \mathbf{X}_o$ $\mathbf{X}_s = (x^*, y^*, z^*)$ $\mathbf{X}_o = (x, y, z)$
Injection Pressure, P		$\mathrm{P_o(t) = P_{o,k}(t)}$ $\mathrm{(k = 1,...,l)}$ (l : Number of injection port)	$P_s(t) = P_{s,k}(t)$ $(k = 1,...,l)$

t : time, Subscript 'o' and 's' : the original and the sample

a_ε, a_K, a_L : Scale factors between the original and the sample

Table 2. Material properties used in the original problem

Reinforcement	Permeability $[K]$	Mat 1	$[K]_{o,1} = \begin{bmatrix} 10\times10^{-10} & 0 \\ 0 & 8\times10^{-10} \end{bmatrix}$ $\mathrm{m^2}$, $\theta = 135^\circ$
		Mat 2	$[\mathrm{K}]_{\mathrm{o,2}} = \begin{bmatrix} 6\times10^{-10} & 0 \\ 0 & 4\times10^{-10} \end{bmatrix}$ $\mathrm{m^2}$, $\theta = 0^\circ$
		Mat 3	$[K]_{o,3} = \begin{bmatrix} 5\times10^{-10} & 0 \\ 0 & 2.5\times10^{-10} \end{bmatrix}$ $\mathrm{m^2}$, $\theta = 45^\circ$
	Porosity ε	Mat 1 Mat 2 Mat 3	$\varepsilon_{o,1} = 0.65$ $\varepsilon_{o,2} = 0.4$ $\varepsilon_{o,3} = 0.5$
Resin	Viscosity, μ		$\mu_o = 0.7$ Pa · sec

θ : Rotation angle of reinforcement between the principal direction and the Cartesian coordinate system

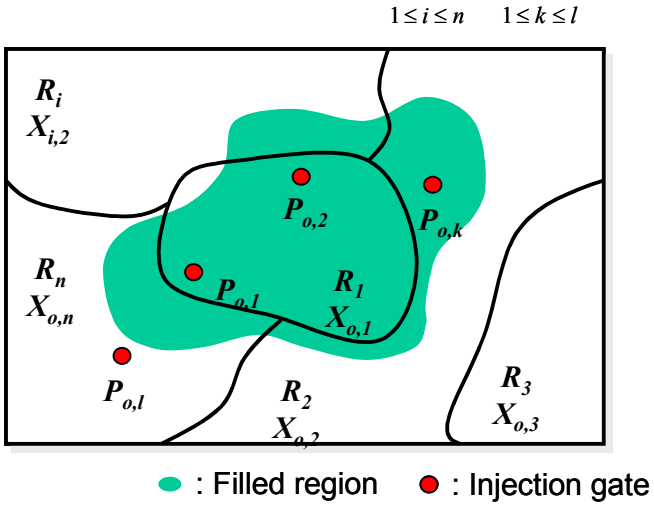

Fig.1 Definitions of properties and variables for deriving similarity relations

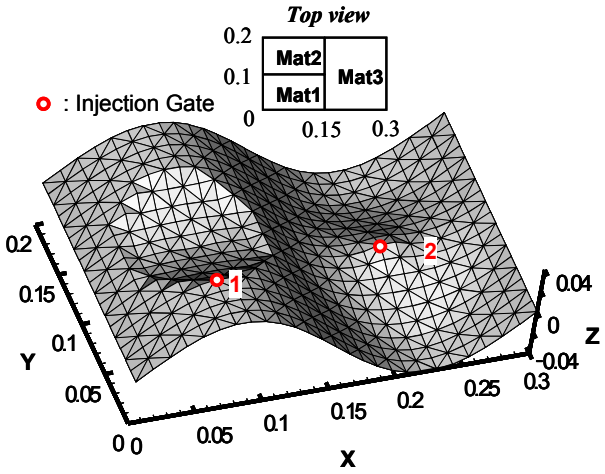

Fig.2 Geometry and mesh for the numerical simulation in the original case

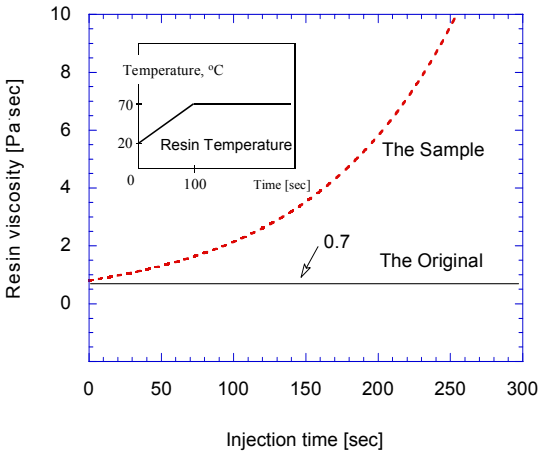

Fig.3 Viscosity variation in the original and sample cases

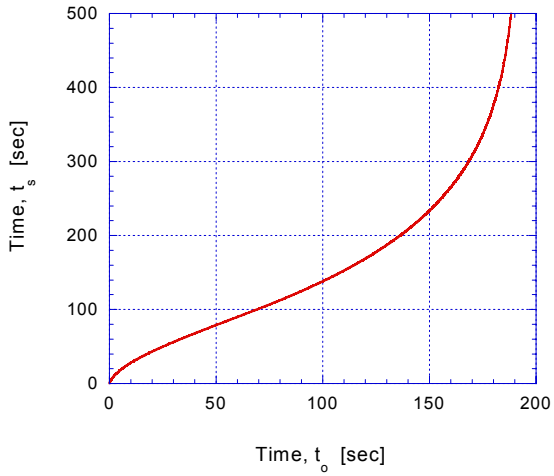

Fig.4 Time scale transformation between

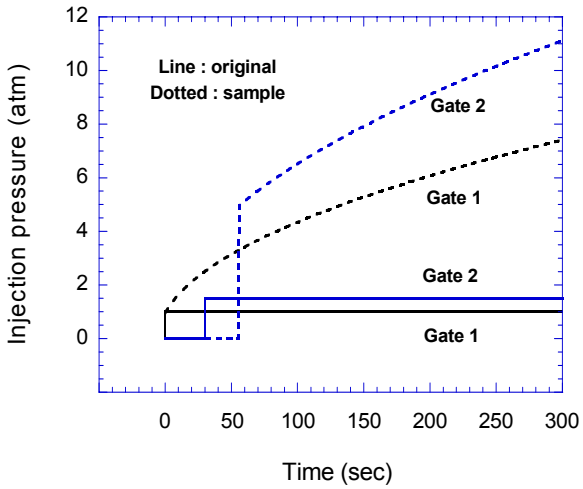

Fig.5 Injection pressures

the original and the sample in the original and sample cases

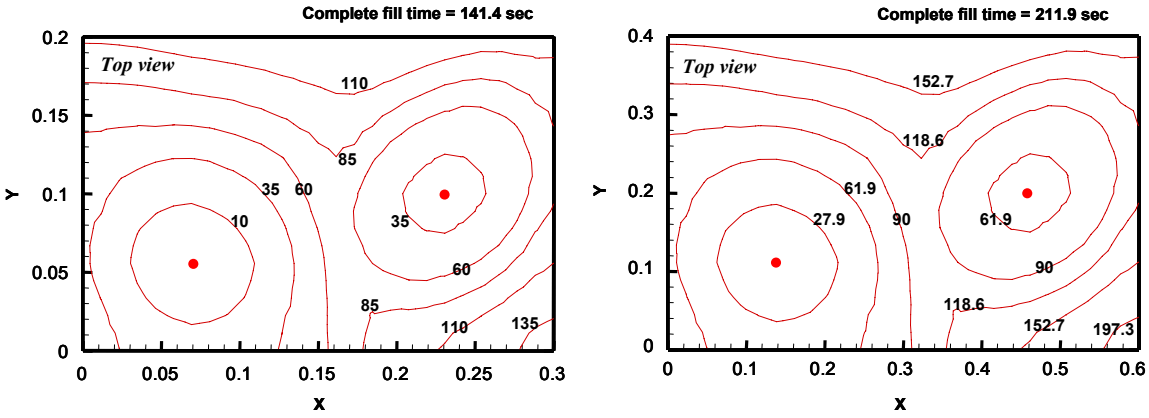

(a) Original problem (b) Sample problem

Fig.6 Comparison of Flow front propagation

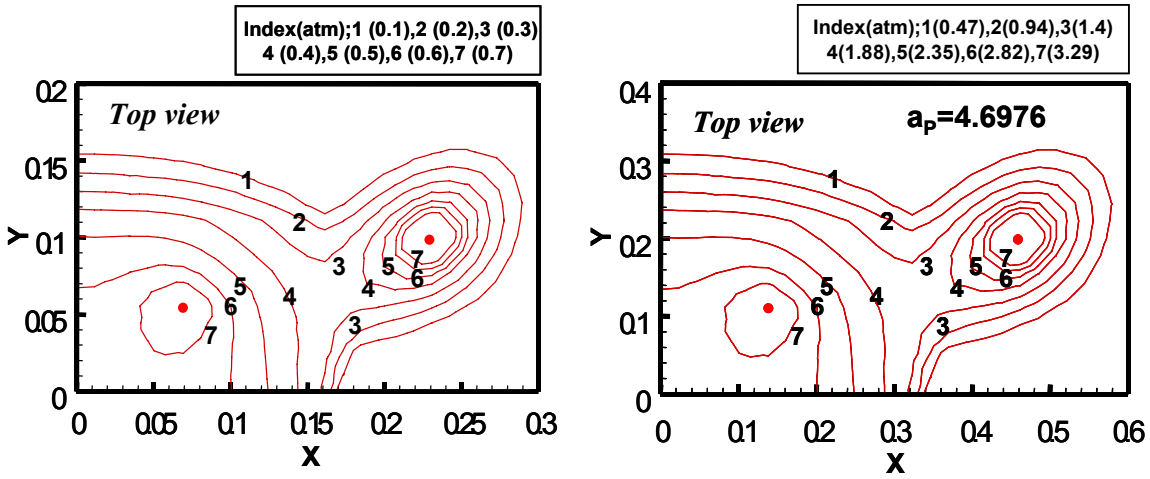

(a) original case (fill time 84.1 sec) (b) the sample case (fill time 117.6 sec)

Fig.7 Numerical result of pressure field

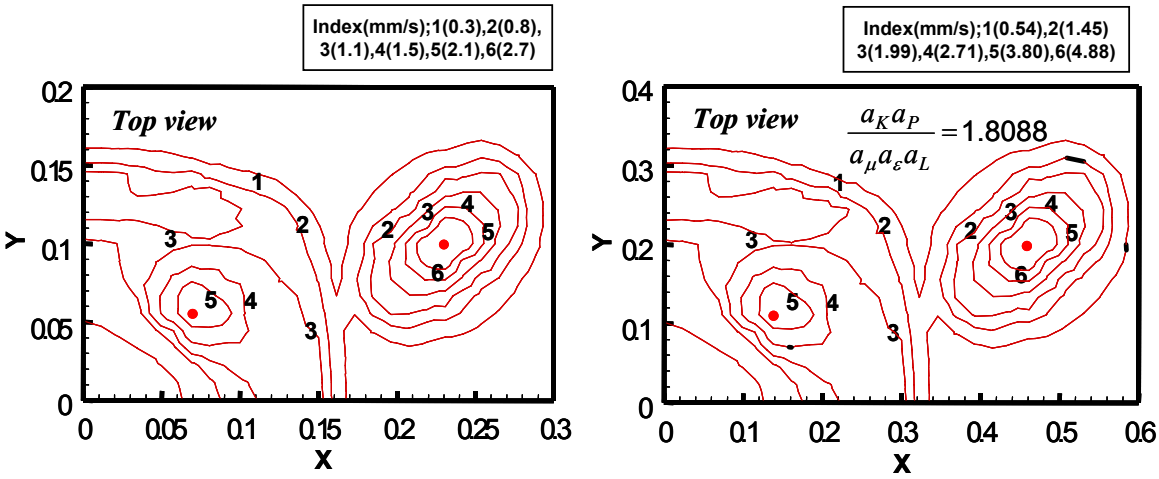

(a) original case (fill time 67.9 sec) (b) sample case (fill time 99.5 sec)

Fig.8 Numerical result of velocity field